INSTITUTE OF PHYSICS PUBLISHING JOURNAL OF PHYSICS B: ATOMIC, MOLECULAR AND OPTICAL PHYSICS

J. Phys. B: At. Mol. Opt. Phys. **35** (2002) 671–689 PII: S0953-4075(02)29633-9

M1/E2 transition rates in Fe X through Fe XIII measured at a heavy-ion storage ring

E Träbert[1,2], G Gwinner[3], A Wolf[3], E J Knystautas[4], H-P Garnir[2] and X Tordoir[2]

[1] Experimentalphysik III, Fakultät für Physik und Astronomie, Ruhr-Universität Bochum, D-44780 Bochum, Germany
[2] IPNAS, Université de Liège, Sart Tilman B-15, B-4000 Liège, Belgium
[3] Max-Planck-Institut für Kernphysik, D-69117 Heidelberg, Germany
[4] Département de physique, Université Laval, Québec, Canada G1K 7P4

E-mail: traebert@ep3.ruhr-uni-bochum.de

Received 8 October 2001, in final form 6 December 2001
Published 31 January 2002
Online at stacks.iop.org/JPhysB/35/671

Abstract

The rates of several electric-dipole forbidden decays of 3p and 3d levels in Cl-, S-, P- and Si-like ions of Fe have been measured optically at a heavy-ion storage ring. In several cases, more than one decay contributes to a given decay curve, which complicates the analysis. The lifetime results, with a precision range from 0.6 to 20%, compare well with some theoretical predictions, but are more precise. They are also more precise than some experimental data from an electrostatic ion trap.

1. Introduction

'Forbidden' lines, spectral lines from transitions that are forbidden by the electric-dipole (E1) transition selection rules, are of great interest since Edlén (1942) identified the famous coronal lines in the visible spectrum of the solar corona with just this type of transition between levels in the ground configurations of highly charged heavy ions. For plasma physics, they opened an observational window into hot plasmas that was to become important several decades later, with the advent of fusion plasma experiments (Edlén 1984). The energies of the low-lying levels of few-electron ions of elements up to the iron group have been systematized among others by Smitt *et al* (Smitt *et al* 1976, Edlén and Smitt 1978) and by Sugar and Corliss (1988), so that the wavelengths of many of the magnetic dipole (M1) and electric quadrupole (E2) transitions are well known.

Under typical coronal conditions, Fe X, the spectrum of the Cl-like ion (17 electrons) of Fe ($Z = 26$) is one of the most prominent spectra. The M1/E2 transition between the fine structure levels of the $3s^2 3p^5$ ground state gives rise to the 'red coronal line' at $\lambda = 637.46$ nm. Such transitions in the ground configurations of various abundant ion species have been exploited

in coronal hole studies (Fisher and Musman 1975), for large-scale temperature diagnostics (Guhathakurta *et al* 1993), and have been observed and analysed in symbiotic stars (Wallerstein and Brugel 1988), Seyfert galaxies (Osterbrock 1981), Supernova remnants (Woodgate *et al* 1974, 1975, Lucke *et al* 1979, 1980, Itoh 1979, Brown *et al* 1988), interstellar absorption lines (Hobbs 1984), cooling flow clusters (Anton *et al* 1991), and so on. Surveys of the required atomic data have been presented elsewhere (Eidelsberg *et al* 1981, Kafatos and Lynch 1980, Lynch and Kafatos 1991). The prospects of similar work extending to the infrared wavelength range have been outlined by Greenhouse *et al* (1993).

For the first excited configuration that involves 3d electrons, however, spectroscopic level information is grossly incomplete. (There are of the order of 30 levels in each of the ions investigated, of which only a few are so long-lived as to be of interest for the present study.) For iron, the heaviest element that appears with a relatively high abundance in the Sun, most of the $3s^2 3p^4 3d$ levels of Fe X are known by now (Sugar and Corliss 1988, Träbert 1998), but only about half of the corresponding $3s^2 3p^3 3d$ levels in the neighbouring Fe XI system (Fritzsche *et al* 2000). Various prominent transitions of Fe X (from low-J $3s^2 3p^4 3d$ levels) fall into the extreme ultraviolet (EUV) range that has been repeatedly studied by ever-better resolving spectrographs on a variety of spacecrafts aimed at the Sun. Some of the high-J levels have only a single E1 decay branch to one of the ground configuration levels. This renders line identification difficult; however, the combination of single-element operation, 'delayed' spectra and charge-state variation offered by beam–foil spectroscopy has enabled some classification work in various Fe ions (Träbert 1998).

Some other high-J levels, however, differ by more than one unit in J from any of the levels of the ground configuration and thus decay only by electric-dipole forbidden transitions. Many of these have most probably been observed, but not identified because of a lack of laboratory comparison data: this lack arises from the fact that the transition rates are lower than the collision rates in most terrestrial light sources, and thus the levels are quenched collisionally. While for Fe X a number of transitions from high-J levels have been identified in the solar corona (Smitt 1977, Edlén and Smitt 1978) at around the same time as calculations have been done in order to systematize the search for such transitions (Mason and Nussbaumer 1977), many of the similarly expected lines in the neighbouring spectra Fe XI through Fe XIII (that also feature high-J levels in the excited 3d configuration) are still missing.

Ion traps with ultrahigh vacuum may eventually solve this experimental problem. Three sets of results from an electrostatic ion trap are available that give lifetimes for ground configuration (3p) and excited configuration (3d) levels in Fe X to Fe XIV (Moehs and Church 1999, Moehs *et al* 2000, 2001). However, measurements using a heavy-ion storage ring (Doerfert *et al* 1997, Träbert *et al* 1999a, 1999b) may well be expected to do better than those with respect to both systematic error and precision of the lifetime determination (this paper).

2. Experiment

Our experiment employed a heavy-ion storage ring (TSR at the Max Planck Institute for Nuclear Physics, at Heidelberg, Germany) using the procedures described previously (Doerfert *et al* 1997, Träbert *et al* 1998, 1999a, 1999b). All ion beams were produced as negative Fe ions from a sputter-type ion source. These ions were then accelerated in the first half of a tandem accelerator, stripped to the desired charge state in a foil stripper, and accelerated further to final energies of about 68 and 100 MeV for Fe^{9+}, 122 MeV for Fe^{10+} and Fe^{11+}, and 143 MeV for Fe^{12+}. For Fe^{13+}, this single-stripping stage technique was considered too inefficient within the technical limits of the given accelerator (the ion yield would have been rather low at the highest energy available). Instead, Fe^{4+} ions were produced in a gas stripper and were further

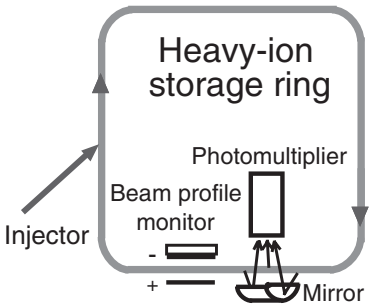

Figure 1. Experimental arrangement. Ions from the injector enter the 55 m circumference storage ring and are kept coasting after the injection ends. Then the optical emission detected by a photomultiplier tube is recorded. The remaining gas ionization (as a measure of the stored ion beam current) is detected by the beam profile monitor.

accelerated to about 28 MeV. These ions were then passed through a thin carbon foil to reach charge state $q = 13+$ for injection into the storage ring. In all cases, only a selected-charge state ion beam was transported to and injected into the storage ring. Multi-turn injection and stacking of the ions over about 30 turns increased the number of stored ions, so that ion currents in the ring reached up to about 50 μA for Fe^{9+}, Fe^{10+} and Fe^{12+}, 100 μA for Fe^{11+}, but only 28 μA for Fe^{13+}. The ions were left coasting for 200 ms to 1 s, depending on the atomic lifetime sought. Then the stored ion beam was dumped and the procedure repeated.

A few per cent fraction of the ion beam was expected to be in excited levels from the stripping and excitation processes that take place inside the injector. The ion beam travels about 100 m from the injector to the ion storage ring, which at these ion energies takes about 6 μs, that is about twice the revolution time of the ions in the storage ring (circumference 55 m). The injection extends over $\approx$0.3 ms; the pulsed magnetic field used to inflect the ions settles down at $\approx$0.8 ms after the start of the injection. After the end of the settling time the ions are stored in stable orbits. The storage time constants (limited by collisional losses) depend on the background gas pressure (here a few times 10^{-11} mbar); they range from about 30 s for Fe^{9+} to 65 s for Fe^{12+}. For Fe^{13+} ions at their relatively low energy (see above), the measured storage time is only about 2.6 s. The actual ion beam current is monitored on-line by a beam profile monitor which detects rest gas ions that are collisionally produced by the circulating ion beam (figure 1). In principle, the ion beam lifetime is important as a systematic correction of the apparent optical decay data, but in the present case this is mostly a 10^{-3} effect and (with two exceptions) negligible. The full injection and settling time is faster than the shortest of the expected radiative lifetimes of present interest, but very long compared to all cascade transitions from higher-lying levels except for those that involve some high-J 3d levels that dominantly decay via M1/E2/M2 transitions.

We have used optical observation in a side-on geometry, through a sapphire window positioned at a distance of 5 cm from the average ion trajectory (figure 1). In order to boost the signal rate, a light collection system was employed (Doerfert *et al* 1997). This simple trough-shaped reflector (of elliptical cross section, with the cylinder axis oriented along the beam trajectory) enhances light collection by about a factor of two. The light was detected by photomultiplier tubes (PMTs) with 25 mm diameter windows and inherent dark rates of one count per second (cps) (solar-blind type EMR 541 Q for UV light) and about 30 cps (bi-alkali type EMR 541 N for visible and near-UV light), respectively. An interference filter centred at 310 nm was used with the EMR 541 N phototube for the observation of the 307 nm line of

Fe XII, and a 530 nm filter for the prominent line in Fe XIV. A red-sensitive EMI 9558B tube cooled to about 0 °C, in combination with a 640 nm filter, was tried for the observation of the principal line in Fe X, but this observation failed because of an insufficient signal in comparison to the dark rate of this photomultiplier at this temperature. Similarly, the observation of the Fe XIV line yielded data, but of insufficient signal on top of the dark rate of the detector, so that a systematic error beyond the statistical uncertainty (which in this case was dominated by the background) cannot be excluded (see below).

The solar-blind EMR 541 Q phototube, in contrast, has an upper wavelength working-range limit near 290 nm; the lower wavelength cut-off is near 180 nm (limited by air in the light path between the storage-ring vessel window and the photomultiplier), or near 160 nm with an evacuated light path. The width of this wavelength interval has led to the observation of several decay components (all in the same ion species and charge state) simultaneously. However, the good statistics obtainable from filterless operation of a low-noise photomultiplier has made it possible to evaluate such composite decay curves. For some of the transitions, wavelengths are not yet well established. Moreover, with several of the expected transition wavelengths being rather closely spaced, filters would reduce the signal rate without necessarily yielding cleaner data. Nevertheless, a single observation in this range has been made with a filter (192 ± 10 nm, transmission 16%, for the Fe^{9+} 191.8 nm lines) which barely permitted a statistically significant lifetime measurement in the face of an ailing ion source that resulted in a stored ion beam current of less than 1 μA particles.

Each detection cycle was started about 1 ms before injection, and events were sorted into 200–1000 bins, each of 0.2–1 ms width. The bin widths were tested by feeding in 1 MHz pulses from a well-stabilized frequency generator. The absolute width was reproduced to better than 4×10^{-4}, with a variation that was less by another order of magnitude. Thus the time base of our experiment is of a negligible uncertainty compared to statistical and evaluational uncertainties.

3. Data evaluation and results

Spectral lines from the long-lived levels of present interest appear throughout the EUV, UV and visible spectral ranges. We presently have no proper means of observation in the EUV. While the 3s–3p transitions within the ground configurations are sufficiently well established and their wavelengths known, much of the 3d shell structure is only available from calculations and educated guesses. Thus the wavelengths of interest that are predicted to lie in the UV and visible ranges are not all known with spectroscopic precision. The calculations indicate that numerous line multiplets overlap, and very-narrow band filters would be required to guarantee the observation of individual level decays in all cases. Not only are such filters of sufficient selectivity and transmission difficult to come by, but in many cases the centre wavelengths of interest cannot even be specified properly in the absence of prior line identifications. Moreover, some of the lines that arise from different upper levels—all in a given ion—are so closely spaced that individual filters are not practical. Turning these problems around, most of the data were recorded with the solar-blind detector, but without using any filter. In this way the signal rate was maximized. This helped to achieve statistically reliable data that could be analysed for the one, two, or three expected lifetime components expected in the wavelength interval covered.

The data sets (for samples, see figures 2–5) were collected and evaluated individually. Nonlinear least-squares fits of one, two or three exponential components (plus a constant background) were tried by applying different algorithms (including user-directed choices of start parameters as well as fully automated routines) to the full data sets, and also to various

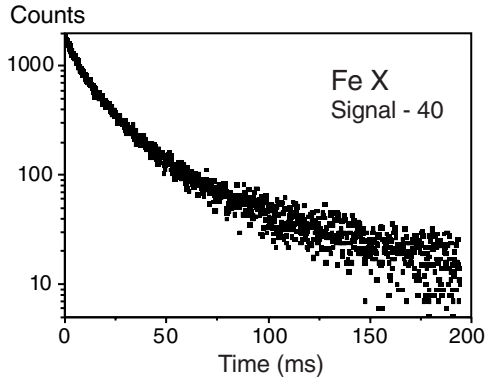

Figure 2. Photon signal (logarithmic scale) obtained with Fe x in the wavelength interval from about 180–290 nm. The data shown represent a collection time of about 36 s per channel. A background contribution of 40 counts has been subtracted from the data shown. Three exponential decay components are needed to fit this decay curve, representing (at least) three 3d levels.

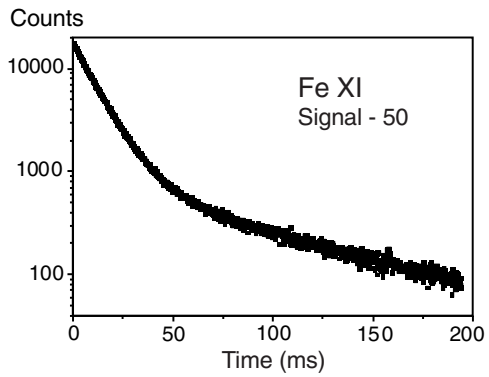

Figure 3. Photon signal (logarithmic scale) obtained with Fe XI in the wavelength interval 180–290 nm. The data shown represent a collection time of about 60 s per channel. A background contribution of 50 counts has been subtracted from the data shown. The decay curve is dominated by the decay of the $3s^2 3p^4\ {}^1D_2$ level. The slow decay component is expected to represent a superposition of the decay signals of the $3s^2 3p^3({}^2P^o)3d\ {}^{1,3}G^o_4$ levels.

subsets: these included truncation of the background tail, which yielded no notable differences, and sequential truncation of up to 20 early data channels (2–20 ms) after the curve maximum. Truncating the very first few channels removes data channels which might be affected by the injection process and the subsequent stabilization of the coasting ion beam in the storage ring. When the evaluation was restricted to data recorded later than 1 ms after the end of the injection, the lifetime results for the low-charge state ions (as a function of starting channel) varied only within the statistical uncertainty of the individual data set. A correction for relativistic time dilation (for example, $\gamma = 1.002\,34$ for 122 MeV ^{56}Fe ions) was applied, but made little difference at the present level of precision. The observed spectral lines make up fine structure intervals of several eV. This is many orders of magnitude larger than any possible Zeeman shifts of the levels in the magnetic fields of the ion beam guidance system. Therefore, any notable effect on the measured atomic lifetimes, by the Zeeman mixing of the levels of interest, can be safely excluded.

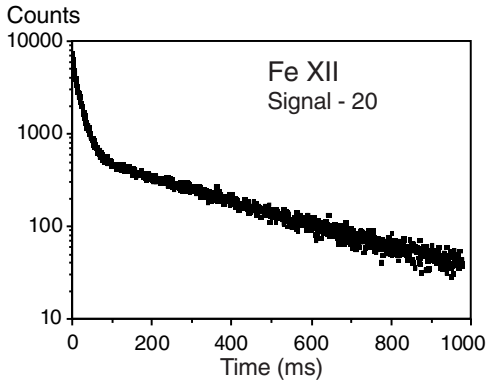

Figure 4. Photon signal (logarithmic scale) obtained with Fe XII in the wavelength interval 180–290 nm. Note the longer storage cycle (1 s) compared to the other measurements (0.2 s). The data shown represent a collection time of about 40 s per channel. A background contribution of 20 counts has been subtracted from the data shown. There are two (relatively) fast and one slow component in this decay curve, all relating to levels in the ground configuration, plus possibly another fast decay component from a 3d level.

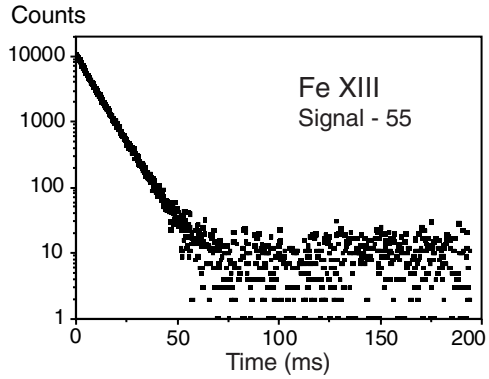

Figure 5. Photon signal (logarithmic scale) obtained with Fe XIII in the wavelength interval from about 180–290 nm. The data shown represent the sum of all data and thus a collection time of about 80 s per channel. A background contribution of 55 counts has been subtracted from the data shown (the fitted background is about 60 counts). To a good approximation, this decay curve is single-exponential, representing the decay of the $3s^2 3p^2\ ^1D_2$ level.

The statistical uncertainty of some of the fit results is extremely small, owing to the high number of signal counts collected (up to 1.6 million in a single decay curve data set, with an almost negligible background contribution). The scatter of the individual results of repeated measurements is fully compatible with the small statistical uncertainty that is smaller than 1% in several of the cases studied. A considerably larger uncertainty arises from the observed shape of some of the decay curves that reveals the presence of several decay components. Some of these are relatively easy to deal with, because they are sufficiently different in time constant, as is the case in Fe X, with three major components of predicted lifetimes near 5, 14 and 58 ms. (Note, however, that several levels are predicted to have almost coincident level lifetime values.) In Fe XI, however, a (weak) 10 ms-cascade is expected to feed a 10 ms-level, and in both Fe XI and Fe XIII (figure 4(*a*)), the $^1S_0$ level lifetime is predicted near 1 ms, with the level feeding the 10 ms (6.5 ms in Fe XIII) $^1D_2$ level via a weak decay branch. This weak decay branch contributes to our signal directly as a blend to the much stronger $^1D_2$ level decay signal, but it also appears

as a growing-in cascade to the signal of the latter. The two appearances were modelled in a simulation, but they could not be disentangled from the experimental decay signal. Thus we have no actual measurement of the two $^1S_0$ level lifetimes (the major decay branches are in the vacuum UV below the cut-off wavelength of the window transparency). Our modelling of all low-lying levels and of some cascade repopulation from hydrogenic levels indicates that the decay curves of all levels of present interest peak about 1 ms after excitation, which again is comparable to the lifetimes of the $^1S_0$ levels in Fe XI and Fe XIII. We have consequently restricted the analysis of these curves to times later than a few milliseconds after injection.

A second problem arises from the longevity of some of the levels in combination with the low dark rate of our solar-blind photomultiplier. By the end of the ion storage cycle, that is close to 200 ms after injection, the signal from those decays has not yet reached the background level. Such a situation leads to ambiguous fits with similar χ^2 values for different combinations of slow decay component and flat background (figures 3, 4). In order to study a near-300 ms lifetime in Fe XII, we therefore lengthened the storage cycle to 1 s (at the cost of a lower injection frequency and thus loss of signal for the faster decay components). Although by that time the signal had not yet disappeared into the background, the fit procedure became much less ambiguous. Fortunately, the data contain data channels that provide an explicit check of the true background: the first channels of each recording show the signal with the old ion sample having been dumped and before the fresh ones are injected. Guided by this measure, the true background can be identified and the data corrected for. This background level is consistent with the true dark rate of this photomultiplier of just below 1 cps.

In all cases we have recorded several independent decay curves, and we derived the final results for the level lifetimes as the weighted means of the individual results. Our final errors represent 1σ-uncertainties (67% confidence limit). The results for the total decay rates were converted to the atomic level lifetimes given in tables 1–5 along with the known or assumed transition wavelengths. In the following, we discuss observations from the data evaluation for the individual ion species. A general discussion of the results follows in the last section.

The Fe^{9+} ion (spectrum Fe x) has two levels in the $3s^23p^5$ ground configuration, a single $3s3p^6$ level, and 27 levels in the $3s^23p^43d$ configuration. Of the latter, seven feature lifetimes in the millisecond range ($^4D_{7/2}$, $^4F_{9/2}$, $^4F_{7/2}$, (^3P) $^2F_{7/2}$, $^2G_{9/2}$, $^2G_{7/2}$, (^1D) $^2F_{7/2}$). This is because the ground configuration levels have a maximum total angular momentum value $J = 3/2$, and therefore no electric-dipole transitions ($\Delta J \leqslant 1$) connect the ground-state levels and these high-J 3d levels. A level scheme has been presented by Huang *et al* (1983).

In Fe x, the transition of primary interest is that within the ground configuration, giving rise to the prominent 'red' coronal line at 637 nm. Decays of the various long-lived 3d levels are expected to appear in all spectral ranges from the EUV to the visible. Unfortunately, none of the photomultipliers available to us at the time yielded enough signal to study the red line. However, while testing red-sensitive PMTs in the section of the storage ring that normally serves for laser-cooling experiments, the solar-blind photomultiplier was available in its usual position (in a different quadrant) for simultaneous observations in the UV range of the spectrum. Operated without a filter and thus sensitive to light of wavelengths from about 180 to about 290 nm, this device yielded data that revealed (at least) three major contributions to the composite decay curve (of about 5, 16 and 60 ms) (figure 2). Theory predicts more than three contributing levels in the UV spectral range; several of these, however, are expected to show level lifetimes near 15 ms that would be virtually indistinguishable from each other. Moreover, some of the decay channels of a given level overlap spectrally with those of others, so that high spectral resolution would be required for individual level decay studies. Such high spectral resolution was not available in this experiment and is generally a problem (at fast ion beams) associated with the solid angle of detection.

Table 1. Predicted and observed decays, and measured lifetimes τ for levels in Fe x. Wavelengths without further reference are approximate and based on observation, indirect evidence (calculated multiplet structure) or calculation (see text). There are other levels with lifetimes in the millisecond range, but they only feature decay branches outside of our wavelength detection range.

Observation band pass 635–645 nm (this work)				
Decay curve component (ms)			Lifetime (ms)	
				Experiment
This work	Upper level	Wavelength (nm)	Predicted	Other work
—	$3s^2 3p^5\ {}^2P^o_{1/2}$	637.46[h]	14.46[a]	13.64 ± 0.25[k]
			14.41[b,h]	
			14.40[c]	
			14.46[e]	
			14.37[f]	
			14.44[g]	
			18.21[i]	
			15.29[j]	
			14.42[k]	
Observation band pass 180–200 and 190–280 nm, respectively, in this work				
16.0 ± 1.6	$3s^2 3p^4(^3P)3d\ {}^2F_{7/2}$	191.8	20.8[d]	
			17.6[i]	
			14.1[j]	
4.6 ± 0.4	$3s^2 3p^4(^1D)3d\ {}^2F_{7/2}$	194.7, 221.5, 226.6,	6.5[d]	
		238.9, 283.8, 286.5	5.22[i]	
			4.9[j]	
58 ± 10	$3s^2 3p^4(^3P)3d\ {}^4F_{7/2}$	293.4	15.1[d]	93 ± 30[k]
			84.0[i]	
			57.9[j]	
			80.0[k]	
—	$3s^2 3p^4(^3P)3d\ {}^2G_{7/2}$	299.1, 353.5	18.6[d]	
			20.6[i]	
			14.0[j]	
—	$3s^2 3p^4(^3P)3d\ {}^4F_{9/2}$	345.5	85.5[d]	85.7 ± 9.2[k]
			91.4[i]	
			80.2[k]	
—	$3s^2 3p^4(^1D)3d\ {}^2G_{9/2}$	302.1	14.5[d]	17.8 ± 3.1[k]
			14.5[i]	
			16.7[k]	

[a] Krueger and Czyzak (1966).
[b] Smith and Wiese (1973).
[c] Kastner (1976).
[d] Mason and Nussbaumer (1977).
[e] Kafatos and Lynch (1980).
[f] Eidelsberg *et al* (1981).
[g] Huang *et al* (1983).
[h] Kaufman and Sugar (1986).
[i] Bhatia and Doschek (1995).
[j] Kohstall *et al* (1999), Dong *et al* (1999).
[k] Moehs *et al* (2000, 2001).

The three lifetimes found by our analysis can be readily assigned to three $3s^2 3p^4 3d\ J = 7/2$ levels (table 1). A fourth such level is expected to radiate near 299 nm, which is very near the long-wavelength end of the detection range of the solar-blind PMT where the quantum efficiency is rather small, so that the contribution of this signal to the overall decay data

Table 2. Predicted and observed decays, and measured lifetimes τ for levels in Fe XI. Wavelengths are approximate and based on observation, indirect evidence (calculated multiplet structure) or calculation (see text). There are other levels with lifetimes in the millisecond range, but they only feature decay branches outside of our wavelength detection range.

Observation band pass 160–280 nm				
Decay curve component (ms)			Lifetime (ms)	
This work	Upper level	Wavelength (nm)	Predicted	Experiment Other work
—	$3s^2 3p^4\ ^1S_0$	146.7, 232.2	0.94–1.12[a–k]	
11.05 ± 0.1	$3s^2 3p^4\ ^1D_2$	264.9, 398.8	10.5[a]	9.86 ± 0.22[m]
			10.0[b,c]	
			12.8[d]	
			9.84[e]	
			9.83[f]	
			9.80[g]	
			11.9[h]	
			9.81[i,k]	
			9.74[j]	
			10.8[l]	
			10.65[m]	
	$3s^2 3p^3(^2D^o)3d\ ^3F^o_4$	234.5, 239.4	10.2[d]	
			9.40[i]	
			7.99[k]	
68 ± 4	$3s^2 3p^3(^2D^o)3d\ ^3G^o_4$	273.9	79.4[d]	
			74.6[i]	
			43.2[k]	
	$3s^2 3p^3(^2P^o)3d\ ^1G^o_4$	279.0	45.7[d]	
			25.7[i]	
			15.9[k]	
	$3s^2 3p^3(^2P^o)3d\ ^3F^o_4$	263.5, 275.0, 292.0	1.63[c]	
			1.63[i]	
			1.5[k]	

[a] McKim–Malville and Berger (1965).
[b] Smith and Wiese (1973).
[c] Smitt *et al* (1976).
[d] Mason and Nussbaumer (1977).
[e] Mendoza and Zeippen (1983).
[f] Biémont and Hansen (1986).
[g] Kaufman and Sugar (1986).
[h] Saloman and Kim (1989).
[i] Bhatia and Doschek (1996).
[j] Chou *et al* (1996).
[k] Fritzsche *et al* (2000).
[l] Bogdanovich (2000).
[m] Moehs *et al* (2001).

must be small at best. For one case of the other three, the assignment has been tested (and supported) in separate measurements using a filter that excluded all but the decays of the (^{3}P) 3d $^2F_{7/2}$ level near 181.8 nm. Furthermore, as the measurement without a filter revealed three major decay components, one of which had not fully decayed within the standard cycle of 200 ms, a measurement over 500 ms (and, incidentally, at another ion energy) was done in order to improve the determination of the long-lived component and thus the three-component

Table 3. Predicted and observed decays (in two observation bands), and measured lifetimes τ for levels in Fe XII. Wavelengths are approximate and based on observation, indirect evidence (calculated multiplet structure), or calculation (see text).

Observation band pass 190–280 nm				
Decay curve component (ms)			Lifetime (ms)	
This work	Upper level	Wavelength (nm)	Predicted	Experiment Other work
306 ± 10	$3s^2 3p^3\ ^2D^o_{5/2}$	217	324[a]	—
			115[b]	
			326[c]	
			294[d]	
			313[e]	
			544[f]	
			314[g]	
			418[h]	
			315.8[j]	
18.0 ± 0.1	$3s^2 3p^3\ ^2D^o_{3/2}$	240.6	18.9[a]	20.35 ± 1.24[i]
			18.9[b]	
			5.0[c]	
			16.8[d]	
			16.0[e]	
			20.8[f]	
			18.4[g]	
			21.8[h]	
			22.57[i]	
			18.5[j]	
1.70 ± 0.08	$3s^2 3p^3\ ^2P^o_{3/2}$	256.7, 290.3	1.61[a]	1.85 ± 0.24[i]
			1.61[b]	
			2.39[c]	
			1.55[d]	
			1.53[e]	
			1.67[f]	
			1.59[g]	
			1.77[h]	
			1.6[j]	
	$3s^2 3p^2(^1D)3d\ ^2G^o_{9/2}$	180, 275	≈ 4[j]	—
Observation band pass 305–315 nm				
4.1 ± 0.12	$3s^2 3p^3\ ^2P^o_{1/2}$	307.3, 356.7	3.84[a]	4.38 ± 0.42[i]
			3.84[b]	
			3.84[c]	
			3.64[d]	
			3.58[e]	
			4.05[f]	
			3.81[g]	
			4.27[h]	
			3.8[j]	

[a] Garstang (1972).
[b] Smith and Wiese (1973).
[c] Smitt *et al* (1976).
[d] Mendoza and Zeippen (1982a).
[e] Huang (1984).
[f] Kaufman and Sugar (1986).
[g] Biémont and Hansen (1985).
[h] Bogdanovich (2000).
[i] Moehs *et al* (2001).
[j] Biémont *et al* (2001).

Table 4. Predicted and observed decays, and measured lifetimes τ for levels in Fe XIII. Wavelengths are approximate.

Observation band pass 190–280 nm				
Decay curve component (ms)			Lifetime (ms)	
This work	Upper level	Wavelength (nm)	Predicted	Experiment Other work
—	$3s^2 3p^2\ ^1S_0$	121.6, 137.1, 230.2	0.85–0.98[a–f]	
8.0 ± 0.1	$3s^2 3p^2\ ^1D_2$	258.0, 338.9	6.29[a]	6.93 ± 0.18[h]
			7.37[b]	
			6.54[c]	
			6.46[d]	
			5.82[e]	
			9.69[f]	
			7.23[h]	
	$3s^2 3p3d\ ^3F^o_4$	62.8, 63.9, 85.9	9.18[g]	

[a] McKim–Malville and Berger (1965).
[b] Flower and Pineau des Forêts (1973).
[c] Smith and Wiese (1973).
[d] Mendoza and Zeippen (1982b).
[e] Huang (1985).
[f] Kaufman and Sugar (1986).
[g] Kohstall *et al* (1998).
[h] Moehs *et al* (2001).

Table 5. Predicted and observed decays, and measured lifetimes τ for the upper fine structure level of the ground state in Fe XIV.

Observation band pass 525–535 nm				
Decay curve component (ms)			Lifetime (ms)	
This work	Upper level	Wavelength (nm)	Predicted	Experiment Other work
18.0 ± 1.2*	$3s^2 3p\ ^2P^o_{3/2}$	530.286[f]	16.50[a]	17.52 ± 0.29[j]
			16.58[b]	
			16.60[c]	
			16.65[d]	
			16.61[e,f]	
			19.8[g]	
			16.66[h]	
			21.38[i]	
			16.57[j]	

[a] Krueger and Czyzak (1966).
[b] Smith and Wiese (1973).
[c] Kastner (1976).
[d] Kafatos and Lynch (1980).
[e] Eidelsberg *et al* (1981).
[f] Kaufman and Sugar (1986).
[g] Froese Fischer and Liu (1986).
[h] Huang (1986).
[i] Bhatia and Kastner (1993).
[j] Moehs *et al* (2000), Moehs *et al* (2001).
* Tentative result, see text.

analysis as well. However, additional spectroscopic confirmation that these levels make up the dominant part of the signal, to be obtained possibly from an electron-beam ion trap (where Doppler broadening is not an issue), would be most welcome.

Further lifetime work in the wavelength range beyond our solar-blind detector would also help to shed more light on this problem. Typical filters applied to narrow down selectively the spectral range that is seen by a detector make sense only after determining the precise transition wavelengths. In several cases, narrow coincidences of lines from different decays are foreseen that will render likely the appearance of multi-component decay curves even when using a filter. Moreover, filters in this UV wavelength range regularly have a fairly low transmission, which severely reduces the signal-to-noise (detector dark rate) ratio. Counteracting this problem by extending the data accumulation time would require considerable allocations of machine time or a notable investment into multiple detectors. Nevertheless, such extensions are feasible, and they would permit us to obtain a 'second opinion' on the lifetimes of those levels that have been covered by the Kingdon trap group (see summary by Moehs *et al* 2001), but not in our present work.

The Fe^{10+} ion (spectrum Fe XI) has five levels in the $3s^23p^4$ ground configuration (the maximum J value is 2), four $3s3p^5$ levels, and 38 levels in the $3s^23p^33d$ configuration. Of the latter, six feature lifetimes in the millisecond range ($^5D^o_4$, ($^2D^o$) $^3F^o_4$, $^3G^o_4$, $^3G^o_5$, $^1G^o_4$, ($^2P^o$) $^3F^o_4$). A level scheme is shown in figure 6. Our data for Fe XI (figure 3) at face value seem to represent a simple case of a two-component decay curve. While the first component (of 11 ms) is readily determined, the lifetime determination of the second component suffers from the aforementioned problem of background versus long-lived decay-curve component. Fits to the decay curve (over a 200 ms data range) return lifetime values between 55 and 72 ms (with 1.5% statistical uncertainties) in correlation with the background level assumed. The additional evidence from the data channels between ion expulsion and fresh injection points to the longer lifetime value. However, this decay component probably represents two levels ($^3G_4$ and $^1G_4$), with major decay branches near 274 and 279 nm, respectively, and predicted lifetimes that range from 80 and 46 ms (Mason and Nussbaumer 1977) to 43 and 16 ms (Fritzsche *et al* 2000). The experimental result points to the first (and earlier) calculation; however, it is practically impossible to separate, in the multi-exponential decay curve analysis, two decay components that differ in their characteristic time constant by only a factor of two—while a third component and some background contribution are present as well. There also is a third 3d level ($^3F_4$) that is expected to contribute, with a predicted lifetime of less than 2 ms. The level population of the 3d level is expected to be lower than that of the dominant $3s^23p^4\ ^1D_2$ level in this decay curve, and we do not recognize its contribution. Our present results are given in table 2.

Future storage-ring experiments at a lower injection frequency may be able to shed more light this case. For the time being, we quote the result with an overall uncertainty that corresponds to about three times the statistical uncertainty. Yet another 3d level, $^3G_5$, has been predicted to feature a lifetime near 100 ms (Mason and Nussbaumer 1977, Bhatia and Doschek 1996, Fritzsche *et al* 2000). This level radiates at two wavelengths (154 and 432 nm) that are not covered here.

The Fe^{11+} ion (spectrum Fe XII) has five levels in the $3s^23p^3$ ground configuration (the maximum J value is 5/2) (figure 7(*a*)), eight $3s3p^4$ levels, and 28 levels in the $3s^23p^23d$ configuration (a level scheme has been presented by Huang (1984)). Of the latter levels, two feature lifetimes in the millisecond range ($^4F_{9/2}$, $^2G_{9/2}$). The $3s^23p^23d\ ^4F_{9/2}$ level has decay branches in the infrared and in the EUV, but none in our detection range. The $3s^23p^23d\ ^2G_{9/2}$ level has decay branches near the wavelength edges of our detection range and will be discussed below.

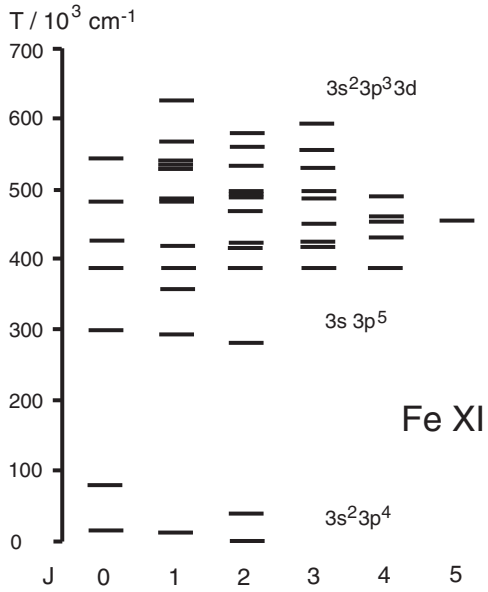

Figure 6. Level scheme of Fe XI. The ground (even parity) and low-lying (odd parity) configurations have levels with a maximum total angular momentum value J of no larger than $J = 2$. Therefore levels with $J = 4$ and 5 in the even-parity $3s^2 3p^3 3d$ configuration cannot decay there by E1 transitions and consequently feature millisecond level lifetimes.

All four excited levels of the ground configuration have been studied for their decay constants in the present work (figure 4, 7(*a*)). However, all higher levels feed the lower levels in the same ground configuration $3s^2 3p^3$, and three levels show their decay components in the same set of observations with the solar-blind detector. Fortunately, the apparent decay time constants are independent of whether a decay is seen directly or as a cascade, and the joint decay curve is therefore characterized by the very same three level lifetimes. A problem arises from the longevity of one of the levels. Even when reducing the injection frequency of the storage ring in order to lengthen the observation time to 1 s per cycle, the longest-lived of the three decay components (1.7, 18, 300 ms) has not disappeared into the background by the end of the cycle (figure 4). These lifetimes are close to what is expected for the $3s^2 3p^3\ ^2P^o_{3/2}$, $^2D^o_{3/2}$ and $^2D^o_{5/2}$ levels, respectively. Fortunately, the data sets have a few channels that show exclusively the background, in the millisecond interval after dumping the old ions and before injecting fresh ones. These data points are distinct enough to determine the background level unequivocally, and consequently the $^2D^o_{5/2}$ level lifetime near 300 ms can be established with confidence. This is the only lifetime for which the ion storage time correction reaches as much as 1% in our experiment.

In our wavelength window, we should be able to detect several of the decay branches of the $3s^2 3p^2 3d\ ^2G_{9/2}$ level, which is long-lived because no M1 decay to the ground configuration is possible. Since this level and its decays were not covered by earlier work, a new calculation has been undertaken by Biémont *et al* (2001) which indicates a level lifetime of the order of 4 ms. Such a set of decays with this lifetime would somewhat affect the observed superposition of the three other long-lived levels, in particular the extraction of the lifetime of the shortest-lived component. However, the expected level population of the excited (3d) level is expected to be much lower than those of the ground configuration levels (that are being fed, for example, by the

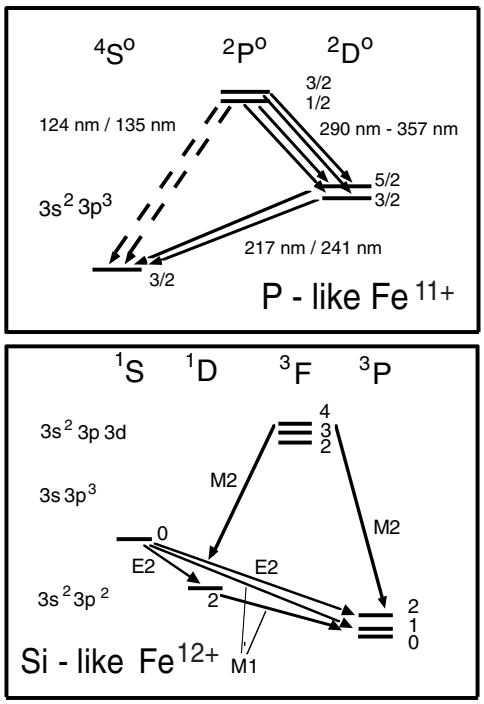

Figure 7. (*a*) Schematics of the levels and transitions (with approximate wavelengths) in the ground configuration of Fe XII. (*b*) Schematics of the levels and transitions of present interest in the ground and low-lying configurations of Fe XIII. In Fe XI, the sequence of the fine structure levels of the ground term, ^{3}P, is inverted in comparison to Fe XIII, but otherwise the situation is very similar.

decays of all other 3d levels). Also, the two predicted major decay branches are at wavelengths near 180 nm (where the transmission of air is low) and near 270 nm (where the detection efficiency of the photomultiplier begins to drop), and thus the contribution of this decay to the present data may be small. However, small is not necessarily negligible, and it is quite possible—although beyond the reliability range of a fit of four exponential decay components to our data—that the (predicted) 4 ms decay component causes a systematic error on the fastest component of our three-exponential analysis. In spite of a small statistical uncertainty of the fit result for the 1.7 ms decay component, this may well represent a superposition of the 4 ms component from the decay of the $3s^2 3p^2 3d\ ^2G_{9/2}$ level with, say, a 1.6 ms component that relates to the $3s^2 3p^3\ ^2P^o_{3/2}$ level. Unconstrained fits of four exponential components failed to return stable results in this case. This was to be expected, since the closeness of the predicted fast components (1.6, 4 and about 16 ms) exceeds the discrimination capability of any regular fit procedure. As a check of principle, the lifetimes of the two slower decay components were then kept fixed at the values obtained from three-component fits, the 4 ms component was admitted at its theoretical lifetime value, and only the lifetime of the fastest decay component (as well as all amplitudes) was fitted, yielding a result near 1.6 ms. Such a lifetime value of 1.6 ms would fit better than the three-component fit result of 1.7 ms to the pattern of lifetimes of all $3s^2 3p^3$ levels as calculated by Biémont *et al* (2001), the theoretical study that otherwise appears to agree best with our findings for Fe XII. However, this is not a positive confirmation of the $3s^2 3p^3\ ^2P^o_{3/2}$ level lifetime as being 1.6 ms, nor of the $3s^2 3p^2 3d\ ^2G_{9/2}$ level lifetime at 4.0 ms. Because of this perceived problem, we quote the 1.7 ms decay component with an uncertainty

of 5% that is much larger than indicated by the fit algorithm. We refrain, however, from estimating a systematic error adjustment. A future direct observation of the $3s^23p^23d\ ^2G_{9/2}$ level decay curve will clarify this point. That experiment will need specific filters—after first finding out the actual wavelengths that cannot be predicted with sufficient reliability by theory.

Only one of the $3s^23p^3$ levels in Fe XII, $^2P^o_{1/2}$, has been observed individually (revealing a lifetime near 4 ms), using a photomultiplier that was sensitive to visible light and thus required a narrow-band filter to reject stray light from other sources. The notable intrinsic dark rate of this detector in combination with the low detector efficiency near the UV end of its working range and the limited filter transmission made us spend more accumulation time on this observation than on all other of the present measurements, but a similar statistical reliability as for the other data remained out of reach. Our results for Fe^{11+} are summarized in table 3.

The Fe^{12+} ion (spectrum Fe XIII) has five levels in the $3s^23p^2$ ground configuration (the maximum J value is 2) (figure 7(*b*)), ten $3s3p^3$ levels, and a single level (out of twelve) in the $3s^23p3d$ configuration that features a lifetime in the millisecond range ($^3F^o_4$). A level scheme has been presented by Huang (1985). The only long-lived level for which a prominent decay branch falls into our detection range is the $3s^23p^2\ ^1D_2$ level in the ground configuration. The decay curves obtained for Fe XIII (figure 5, table 4) appear as a seemingly single-exponential decay that is easily analysed to yield a 8.0 ms lifetime of the $3s^23p^2\ ^1D_2$ level, a result that is close to typical predictions and carries a statistical uncertainty of much less than 1%. Moehs *et al* have found a lifetime of just under 7 ms and also assigned a small uncertainty to it. This difference of the experimental lifetime results indicates a very large discrepancy, considering the minute statistical uncertainties, and it is necessary to investigate whether there might be some physics problem hidden behind these discrepancies. We have already mentioned above that the $3s^23p^2\ ^1S_0$ level contributes a weak cascade (of a lifetime just under 1 ms) into this level that also would appear as a blend. Furthermore, there is the $3s^23p3d\ ^3F^o_4$ level that is long-lived because there is no level in the lower configurations that it can decay to except by M2 transition (or even higher multipole order). At 9.18 ms (Kohstall *et al* 1998), the prediction for the lifetime of this level is very close to the lifetime of the $^1D_2$ level, and one cannot expect to distinguish the two components from the present data, even as they are statistically much more reliable than those presented by Moehs *et al* (2000, 2001). One question is whether there is any sign of this cascade, and a second is what would need to be done to measure the cascade lifetime. Knowing the latter would help in determining the $3s^23p^2\ ^1D_2$ level lifetime by constrained fits.

Direct observation of the $^3F^o_4$ level decay requires observation in the EUV, near 25 nm (decay to $3s^23p^2\ ^3P_2$), near 63 nm (decay to $3s3p^3\ ^3D_{2,3}$), or near 86 nm (decay to $3s3p^3\ ^3P_2$). All of these are beyond our present means, since they would require a windowless detector inside the storage-ring vacuum vessel.

However, we note a slight deviation of the decay data from a truly single-component fit curve that points to either a blend or a cascade with a lifetime near the principal one. A two-exponential fit to the data results in one major component of (8.4 ± 0.4) ms (where the 5% uncertainty reflects the scatter of the solutions of the two-component fit), and a second, weaker component of about 5 ms ($\pm$10%). The amplitude of the faster component of the unconstrained two-component fit would point to a level with an initial population that is five to ten times lower than the other (or that a correspondingly small branch fraction leads to the signal we observe). If this 5 ms lifetime was real, the identity of this level—in the same ion—would be mysterious. If the 5 ms decay component was from a faster cascade feeding the level of interest, it would show as a growing-in cascade, with its characteristic shape known from many beam–foil observations. However, this signature is absent. We therefore conclude that the two decay components represent the $3s^23p^2\ ^1D_2$ level decay of interest with a lifetime of just below 8 ms, and its slightly slower and markedly weaker cascade repopulation from the

$3s^2 3p3d\ {}^3F^o_4$ level with a level lifetime just above 8 ms. However, such a close pair of lifetime components cannot reliably be determined from any multi-exponential fit.

An educated guess about the relative amplitudes of the two components appears to be the only available tool to narrow down the combination of lifetimes that would yield the observed curve. Based on the branch fractions calculated by Kohstall *et al* (1998) it appears likely that only a very small fraction of the $3s^2 3p3d\ {}^3F^o_4$ level population eventually reaches the $3s^2 3p^2\ {}^1D_2$ level. Introducing a weak component (less than 10% of the decay curve amplitude) with the predicted lifetime of the cascade level (or other lifetime values up to 10 ms) into a constrained fit, restores the (8.0 ± 0.1) ms result now for the major component, but with an uncertainty that reflects the range of results of various constrained fits and is a factor of five larger than the statistical uncertainty of each of the individual single-component fits. We note that at a higher relative background level, the deviation from a true single-exponential curve would not be recognizable—and this might explain why Moehs *et al* (2000, 2001) do not report such a case from their observations.

The Fe^{13+} ion (spectrum Fe XIV) has two levels in the $3s^2 3p$ ground configuration (connected by the astrophysically useful 'green' corona line; the maximum J value is 3/2), various $3s3p^2$ levels (among which the ${}^4P$ levels with their multi-nanosecond lifetimes are the longest-lived), and the relatively long-lived $3s3p3d\ {}^4F^o_J$ levels. Lifetime values of two of the three $3s3p^2\ {}^4P$ levels and of three of the four $3s3p3d\ {}^4F^o$ levels have been obtained by beam–foil spectroscopy (Träbert *et al* 1988, 1993). A level scheme for Fe^{13+} has been presented by Huang (1986) based on MCDF calculations. Very recently, Gupta and Msezane (2001) have extended the calculated data by their CIV3 calculations, but the results presented do not cover the lifetime of the $3s3p3d\ {}^4F^o_{9/2}$ level that may be as long as in the millisecond range. For this level lifetime we have not found any published explicit prediction.

We have already mentioned the problem of too little signal on the 530 nm line in comparison to the dark rate of the available photomultiplier. Thus the decay curve (with an integrated true signal above background of almost 10^5 counts) was dominated by the statistical fluctuations of the underlying integrated dark rate (of more than 10^6 counts within three decay times of the true light signal). This rendered the lifetime result from a single-exponential fit (plus background) rather sensitive to the actual start channel used. Even as a statistical error of only 2% was obtained for the lifetime value, a larger, unrecognized systematic problem of evaluating such background-dominated data was assumed, because the results changed with the counting statistics and the somewhat varying signal-to-background ratio during the experiment. This is in contrast to all our other data that are signal-dominated, with the exception of the slight problem mentioned for the one other background-heavy data set, in Fe XIII (mentioned above). Our present data point to a lifetime value that is 10% higher than the bulk of the predictions, a deviation that is unlikely to be correct. We note that the Kingdon trap result also deviates from the theoretical predictions (although less than our present preliminary result). We also note that an unspecified background was subtracted from those data before further analysis (Moehs *et al* 2000, 2001), which suggests that a similar systematic error of the evaluation may be present in that other experiment. A better signal-to-noise ratio will be needed in order to perform a storage-ring experiment that will settle this case. Such an improvement, in particular for Fe^{13+} (an ion at the performance limit of the present injector), may be expected from the planned upgrade of the Heidelberg TSR injector system that should provide much higher ion beam currents than are presently available.

4. Discussion and outlook

The present lifetime data on ground configuration and low-lying levels of Fe X through Fe XIII that are sensitive to M1, E2 or M2 decays are only the third such experimental data set for

those Fe ions that are of solar coronal interest. Both earlier experiments on Fe X used an electrostatic ion trap and found data that either disagreed with theory (Moehs and Church 1999) or featured just a few results with uncertainties from 10 to 30% (Moehs *et al* 2000), which are of limited value. This uncertainty is particularly important if one decay component derived from one observation is then used to adjust and interpret fit results obtained on another data set (Moehs *et al* 2000). The present storage-ring experiment, in contrast, has used a well-proven technique that suffers significantly less from systematic uncertainties relating to ion storage time and collisional losses (Träbert *et al* 1999a) than the work at the electrostatic ion trap. Moreover, in most of the cases covered, the storage-ring measurement reached a much higher statistical data quality (more systems covered, almost no detector background, negligible systematic error of the experimental technique, about a factor of 100 more signal). However, the high statistical quality also revealed some complexities inherent in our mostly broadband observations that would have gone unheeded with poorer data. It is maybe because of this that some of our results differ from those obtained with an electrostatic (Kingdon-type) ion trap, which were last summarized by Moehs *et al* (2001).

The resulting lifetime values are in reasonable agreement with some of the predictions from theoretical calculations (see tables 1–5 and Fuhr *et al* (1988)). However, no consistent pattern emerges from the comparison with theory, since different levels—even of the same configuration—appear not to be equally well represented by a given theoretical treatment. In some cases theoretical predictions scatter by a factor of three; in other cases the scatter is small, but the typical predictions do not necessarily agree with the experimental findings. For Fe XII we note that we have obtained lifetime values for all 3p levels and find reasonable agreement for all with the results of several calculations. Most of the predictions for the lifetime of the $^1S_0$ level in the ground configurations of Fe XI and Fe XIII agree pretty well with each other. Because the dominant decay branch of this level in both ions has a wavelength below 150 nm, this level lifetime will become accessible to experiment only after implementing a detection system that avoids the sapphire windows on the storage-ring vessel. For the $^1D_2$ level in both ions we find our lifetime results to be consistently longer than the bulk of the predictions as well as the results presented by the experimental competition. Typical systematic errors shorten the apparent lifetime.

Also, the theoretical results available for long-lived 3d levels are sparse and have generally not been done with a precision higher than is required for an orientation, or level calculations have been done and M1/E2 decay channels included, but not the M2 decays that are important for the highest-J levels. The problem of many unconfirmed 3d level positions contributes to this uncertainty. Because the ground configurations are firmly established, their experimentally determined level values can be employed to scale the theoretical transition rates (M1 transition rates scale with the third power of the transition energy, E2 transition rates with the fifth) for these transitions within the ground configuration. Consequently most predictions take guidance from experimental level energy data and may thus reduce some of their scatter and uncertainty. Such reference data are not available for many of the high-J 3d levels of present interest. However, it should also be noted that most of our measurements of 3d level decays have been done without actual wavelength measurements, relying on calculated level schemes that have been somewhat adjusted to a few experimentally known levels.

The proper line identifications of many 3d level decays in the available solar spectra remain an unsolved problem for now. A third type of ion trap (beyond the electrostatic trap and the heavy-ion storage ring), the electron-beam ion trap, appears to be more suitable than the first two for obtaining the missing laboratory wavelength data, by virtue of the stored ions being plenty and practically at rest (and it might be used to also add some more lifetime data (Träbert *et al* 2000)). For the actual lifetime measurements on Fe ions of individual charge

states, however, the heavy-ion storage ring technique has shown its enormous potential. The preparation of a high-current ion injector at TSR Heidelberg will soon enhance the lifetime measurement capabilities so that various optical transitions will become measurable with much better reliability.

Acknowledgments

We are happy to acknowledge the dedicated technical support by the TSR group, in particular by M Grieser, K Horn and R Repnow. HPG, EJK, ET and XT acknowledge with pleasure the hospitality of the Max Planck Institute for Nuclear Physics. Travel support by the Deutsche Forschungsgemeinschaft (DFG) (ET) and by Université de Liège (HPG, XT) is gratefully acknowledged, as well as support by NSERC (Canada) to EJK and ET (via E H Pinnington (Edmonton, AB, Canada)). We also acknowledge the loan of some optical system components by P Beiersdorfer (Livermore, CA, USA), A G Calamai (Boone, NC, USA), and J Kowalski (Heidelberg, Germany), and the helpful provision before publication of calculated lifetime values for various ions by P O Bogdanovich, and for Fe XII by E Biémont, P Palmeri, P Quinet and C J Zeippen.

References

Anton K, Wagner S and Appenzeller I 1991 *Astron. Astrophys.* **246** L51
Bhatia A K and Doschek G A 1995 *At. Data Nucl. Data Tables* **60** 97
Bhatia A K and Doschek G A 1996 *At. Data Nucl. Data Tables* **64** 183
Bhatia A K and Kastner S O 1993 *J. Quant. Spectrosc. Radiat. Transfer* **49** 609
Biémont E and Hansen J E 1985 *Phys. Scr.* **31** 509
Biémont E and Hansen J E 1986 *Phys. Scr.* **34** 116
Biémont E, Palmeri P, Quinet P, Zeippen C J and Träbert E 2001 *Eur. Phys. J.* D to be published
Bogdanovich P O 2000 Private communication
Brown L W, Woodgate B E and Petre R 1988 *Astrophys. J.* **334** 852
Chou H-S, Chang J-Y, Chang Y-H and Huang K-N 1996 *At. Data Nucl. Data Tables* **62** 77
Doerfert J, Träbert E, Wolf A, Schwalm D and Uwira O 1997 *Phys. Rev. Lett.* **78** 4355
Dong C, Fritzsche S, Fricke B and Sepp W-D 1999 *Mon. Not. R. Astron. Soc.* **307** 809
Edlén B 1942 *Z. Astrophys.* **22** 30
Edlén B 1984 *Phys. Scr.* T **8** 5
Edlén B and Smitt R 1978 *Sol. Phys.* **57** 329
Eidelsberg M, Crifo-Magnant F and Zeippen C J 1981 *Astron. Astrophys. Suppl.* **43** 455
Fisher R and Musman S 1975 *Astrophys. J.* **195** 801
Flower D R and Pineau des Forêts G 1973 *Astron. Astrophys.* **24** 181
Fritzsche S, Dong C Z and Träbert E 2000 *Mon. Not. R. Astron. Soc.* **318** 263
Froese Fischer C and Liu B 1986 *At. Data Nucl. Data Tables* **34** 261
Fuhr J R, Martin G A and Wiese W L 1988 *J. Phys. Chem. Ref. Data* **17** (Suppl 4) 493
Garstang R H 1972 *Opt. Pura Apl.* **5** 192
Greenhouse M A, Feldman U, Smith H A, Klapisch M, Bhatia A K and Bar-Shalom A 1993 *Astrophys. J. Suppl.* **88** 23
Guhathakurta M, Fisher R R and Altrock R C 1993 *Astrophys. J.* **414** L145
Gupta G P and Msezane A Z 2001 *J. Phys. B: At. Mol. Opt. Phys.* **34** 4217
Hobbs L M 1984 *Astrophys. J.* **284** L47
Huang K-N 1984 *At. Data Nucl. Data Tables* **30** 313
Huang K-N 1985 *At. Data Nucl. Data Tables* **32** 503
Huang K-N 1986 *At. Data Nucl. Data Tables* **34** 1
Huang K-N, Kim Y-K, Cheng K T and Desclaux J P 1983 *At. Data Nucl. Data Tables* **28** 355
Itoh H 1979 *Nature* **281** 656
Kafatos M and Lynch J P 1980 *Astrophys. J. Suppl.* **42** 611
Kastner S O 1976 *Sol. Phys.* **46** 179

Kaufman V and Sugar J 1986 *J. Phys. Chem. Ref. Data* **15** 321
Kohstall C, Fritzsche S, Fricke B and Sepp W-D 1998 *At. Data Nucl. Data Tables* **70** 63
Kohstall C, Fritzsche S, Fricke B, Sepp W-D and Träbert E 1999 *Phys. Scr.* T **80** 482
Krueger T K and Czyzak S J 1966 *Astrophys. J.* **144** 1194
Krueger T K and Czyzak S J 1967 *Astrophys. J.* **149** 237 erratum
Lucke R L, Gull T R, Woodgate B E and Socker D G 1980 *Astrophys. J.* **235** 882
Lucke R L, Woodgate B E, Culhane J L, Socker D G and Zarnecki J C 1979 *Astrophys. J.* **228** 763
Lynch J P and Kafatos M 1991 *Astrophys. J. Suppl.* **76** 1169
Mason H E and Nussbaumer H 1977 *Astron. Astrophys.* **54** 547
McKim-Malville J and Berger R A 1965 *Planet. Space Sci.* **13** 1131
Mendoza C and Zeippen C J 1982a *Mon. Not. R. Astron. Soc.* **198** 127
Mendoza C and Zeippen C J 1982b *Mon. Not. R. Astron. Soc.* **199** 1025
Mendoza C and Zeippen C J 1983 *Mon. Not. R. Astron. Soc.* **202** 981
Moehs D P, Bhatti M I and Church D A 2001 *Phys. Rev.* A **63** 032515
Moehs D P and Church D A 1999 *Astrophys. J.* **516** L111
Moehs D P, Church D A, Bhatti M I and Perger W F 2000 *Phys. Rev. Lett.* **84** 38
Osterbrock D E 1981 *Astrophys. J.* **246** 696
Saloman E B and Kim Y-K 1989 *At. Data Nucl. Data Tables* **41** 339
Smith M W and Wiese W L 1973 *J. Phys. Chem. Ref. Data* **2** 85
Smitt R 1977 *Sol. Phys.* **51** 113
Smitt R, Svensson L Å and Outred M 1976 *Phys. Scr.* **13** 293
Sugar J and Corliss C 1987 *Mon. Not. R. Astron. Soc.* **227** 27p
Sugar J and Corliss C 1988 *J. Phys. Chem. Ref. Data* **14** Suppl. 2
Träbert E 1998 *Mon. Not. R. Astron. Soc.* **297** 399
Träbert E, Beiersdorfer P, Utter S B, Brown G V, Harris C L, Neill P A, Savin D W and Smith A J 2000 *Astrophys. J.* **541** 506
Träbert E, Gwinner G, Wolf A, Tordoir X and Calamai A G 1999 *Phys. Lett.* A **264** 311
Träbert E, Heckmann P H, Hutton R and Martinson I 1988 *J. Opt. Soc. Am.* B **5** 2173
Träbert E, Wagner C, Heckmann P H, Möller G and Brage T 1993 *Phys. Scr.* **48** 593
Träbert E, Wolf A, Linkemann J and Tordoir X 1999 *J. Phys. B: At. Mol. Opt. Phys.* **32** 537
Träbert E, Wolf A, Pinnington E H, Linkemann J, Knystautas E J, Curtis A, Bhattacharya N and Berry H G 1998 *Can. J. Phys.* **76** 899
Wallerstein G and Brugel E W 1988 *Astron. Astrophys.* **197** 182
Woodgate B E, Angel J R P and Kirshner R P 1975 *Astrophys. J.* **200** 715
Woodgate B E, Stockman H S Angel J R P and Kirshner R P 1974 *Astrophys. J.* **188** L79